JOURNAL OF SOLID STATE CHEMISTRY 46, 132–137 (1983)

The Site Distribution of Ti and V and the Metal–Metal Interaction in the Ternary System $(V,Ti)_5S_8$

HIROSHI NOZAKI, MASANOBU SAEKI, MITSUKO ONODA, AND YOSHITO ONODA

National Institute for Research in Inorganic Materials, 1-1 Namiki, Sakura-mura, Niihari-gun, Ibaraki, 305, Japan

Received June 1, 1982; in revised form August 20, 1982

The phase relations of the ternary system $V_{1-x}Ti_xS_{1.57}$ are presented on the basis of X-ray diffractometry. The site distribution of Ti and V atoms in the structure is clarified through an NMR absorption study at room temperature. The phase relations and the site distribution of Ti and V, which appear to be closely related to each other, are discussed in terms of the metal–metal interaction of the face-shared octahedra in the metal-deficient distorted NiAs structure.

Introduction

Most of the 3*d*-transition metal monosulfides crystallize to form the NiAs-type or the distorted NiAs-like structures. The face-shared octahedra of the structure make the metal–metal distance along the *c* axis so short that it may be considered that the metal–metal interaction along the *c* axis yields a considerable effect on the stability of the structure. Vanadium sulfides and titanium sulfides have a wide range of continuum from the NiAs-type to the CdI_2-type structures, and the metal–metal interaction of the face-shared octahedra changes depending on the composition in the MS–MS_2 series (*1*). It has been suggested in a previous study of $V_{1-x}Ti_xS_{1.40}$ ($0 \leq x \leq 1.0$) that *d*-electrons on particular sites of vanadiums have a tendency to localize when the vanadium atoms have titanium atoms as nearest neighbors along the *c* axis (*2*). It has also been suggested that Ti atoms preferentially occupy the metal sites in the metal-full layers of the structure rather than the V atoms and the site distribution of Ti and V atoms mainly depends on the metal–metal interaction between the nearest neighbors along the *c* axis.

In this paper, the phase relations of the ternary system $V_{1-x}Ti_xS_{1.57}$ ($0 \leq x \leq 1.0$) are studied through X-ray diffractometry, and the site distribution of Ti and V in the structures of the ternary system is also investigated through NMR absorption of ^{51}V nuclei. We find that the phase relations depend on the site distribution of the metals, which supports the previous results with $V_{1-x}Ti_xS_{1.40}$. It is also suggested that the metal–metal interaction of the face-shared octahedra of the structure significantly affects the phase relations and the site distribution of the system.

Vanadium sulfides and titanium sulfides crystallize in a different way in the MS-MS_2 series. The compound $VS_{1.57}$ ($x = 0$ in $V_{1-x}Ti_xS_{1.57}$) belongs to the V_5S_8 phase, a representative phase in the V–S system. The structure of V_5S_8 is a metal-deficient NiAs-like structure in which vanadium

0022-4596/83/010132-06$03.00/0

metal vacancies are involved in every second layer of vanadium and, at least at room temperature, these vacancies take an ordered state, resulting in a monoclinic structure (*3*). If the metal vacancies in every second layer of vanadium of V_5S_8 change to take a disordered state within the layer, the V_5S_8 structure changes into a metal-excess CdI_2-type structure which occurs in an intermediate region of composition of $V_{1-x}Ti_xS_{1.57}$. The stacking of sulfur layers is hexagonal close packed for the entire composition range between VS and VS_2 as well as in V_5S_8 and also in the metal-excess CdI_2 phase of $V_{1-x}Ti_xS_{1.57}$. On the other hand, titanium sulfides take a great variety of sulfur packings other than the hexagonal close-packed one except for the compounds TiS and TiS_2 (*4, 5*). Near the composition of $TiS_{1.57}$, there exist several phases with different sulfur packings, that is, Ti_2S_3 (4H-type) (*6, 7*), Ti_5S_8 (12R-type) (*8*), and Ti_5S_8 (2H-type) (*9*). It was suggested that this complex situation is due to the differences between the methods of preparation, i.e., the material history (*9*). In the last two compounds, metal-vacancy orderings were observed within the metal layers (*10, 11*). The same V_5S_8 structure has been found in $TiS_{1.62}$ crystals, which belongs to Ti_5S_8 (2H-type) (*12*). The phase Ti_2S_3, which is made by the present method of preparation, has a sulfur packing of a sequence of ABAC (called 4H-type in Ramsdell notation) and titanium vacancies are also involved in every second layer of titanium, but near the composition of $TiS_{1.57}$, they take a disordered state within the layer (*7*). The metal arrangement of the V_5S_8 phase, the metal-excess CdI_2 phase, and the Ti_2S_3 phase are shown in Fig. 1, where the intervening sulfur layers are omitted for clarity. As seen in the figure, there exist three sorts of metal sites in the V_5S_8 structure, that is, the V_I site in the metal-deficient layer and V_{II} and V_{III} sites in the metal-full layer. It should be noted that the numbers of nearest-neighbor metals along the *c* axis are different from each other among the three sites.

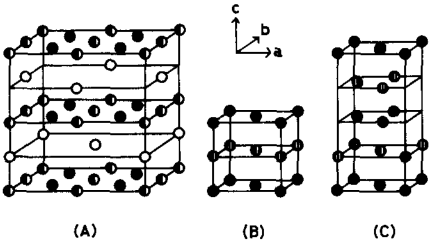

FIG. 1. Schematic arrangements of metal atoms in V_5S_8 (A), metal-excess CdI_2 (B), and 4H-Ti_2S_3(C) structures, where the intervening sufur layers are omitted for clarity. Open and striped circles lie in the metal-deficient layers. In (A), open circles represent the V_I sites and half-solid and solid circles the V_{II} and V_{III} sites, respectively. In (B) and (C), striped circles represent the metal sites, three-quarters of which are vacant with random distribution within the layers. The stacking of sulfur layers in (C) is the ABAC type different from the hexagonal close packing in (A) and (B).

Experimental

Powder samples, $V_{1-x}Ti_xS_{1.57}$, were prepared by heating calculated mixtures of $VS_{1.57}$ and $TiS_{1.57}$ in evacuated silica tubes at 900°C for several days followed by quenching in water. Some samples with composition near $x = 0$ were slowly cooled from 900°C to avoid sulfur loss because of the high sulfur vapor pressure of the samples at high temperatures. Preparation and chemical analysis of the starting materials, $VS_{1.57}$ and $TiS_{1.57}$, were made according to the same procedures as in the previous studies (*4, 13*). Chemical analysis of ternary $V_{1-x}Ti_xS_{1.57}$ was also performed photometrically and gravimetrically as described in Ref. (*14*). The uncertainties in the chemical composition of the specimens can be given as ± 0.02 for x and ± 0.03 for y values in $V_{1-x}Ti_xS_y$. X-Ray diffraction measurements were performed using Cu$K\alpha$ radiation with a Ni filter. Lattice parameters were obtained by the least-squares method.

The NMR absorption study was made using a Bruker SWL40 wideline spectrometer. The spectra were obtained in the form of derivative curves and were integrated by a Tracor Northern NS570A signal analyzer. They were taken at 297K at two frequencies, 10.5 MHz with a 1-kG magnetic field scan and 20.8 MHz with a 500-G scan, respectively (*15*). Resonance shifts were measured with respect to an aqueous solution of NH_4VO_3. The composition for $x = 0$ used in the NMR experiments was not $VS_{1.57}$ but $VS_{1.56}$ in the system $V_{1-x}Ti_xS_{1.57}$.

Experimental Results

The X-ray diffraction patterns showed that there were four different phase regions; these were the monoclinic phase of V_5S_8 type ($0 \leq x \leq 0.4$), the trigonal phase of the metal-excess CdI_2 type ($0.4 < x < 0.8$), the hexagonal phase of Ti_2S_3 type ($0.8 < x \leq 1.0$), and a mixed region of both phases, CdI_2 type and Ti_2S_3 type ($x = 0.8$). The composition dependence of the parameters of the unit cell are summarized in Fig. 2. In the figure, the a and b parameters refer to the orthohexagonal representation of the basic hexagonal cell. For $VS_{1.57}$, $a = 2\sqrt{3}a_{\text{hex}} = 11.3952(5)$ Å, $b = 2a_{\text{hex}} = 6.6637(4)$ Å, $c = 2c_{\text{hex}} = 11.3106(5)$ Å, $\beta = 91° 27'(1')$, and for $TiS_{1.57}$, $a' = a_{\text{hex}} = 3.410(2)$ Å, $c' = 2c_{\text{hex}} = 11.394(7)$ Å. It is seen that the unit cell volume increases with increasing Ti content, probably due to the difference of the ionic radii of V and Ti. The monoclinic distortion within the V_5S_8 phase decreases with increasing x and disappears in the metal-excess CdI_2 phase in which metal vacancies take a disordered state within the layers. The large gap of the c parameters at $x = 0.8$ is due to the change of the sulfur packing from AB type (hexagonal close packing) to ABAC-type packing.

Integrated absorption profiles of ^{51}V NMR are shown in Fig. 3 at some compositions of $V_{1-x}Ti_xS_{1.57}$. The spectra were taken by using a frequency of 10.5 MHz at 297K. In the figure, the spectrum for $VS_{1.56}$ ($x = 0$) consists of two peaks for the ^{51}V nuclei; one, called the type 2 peak, is at about 9.4 kG and originates from the vanadium atoms at the V_{II} and V_{III} sites in the metal-full layers, as assigned by previous authors (*16*), in which vanadium atoms

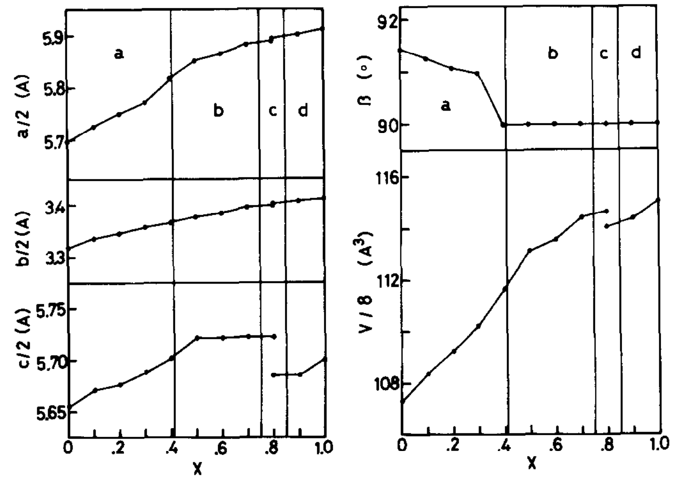

FIG. 2. Composition dependence of lattice parameters in $V_{1-x}Ti_xS_{1.57}$. There exist four regions, and these are the V_5S_8 phase (a); the metal-excess CdI_2 phase (b), a mixed region of two phases; the metal-excess CdI_2 and the Ti_2S_3 phases (c); and the Ti_2S_3 phase (d).

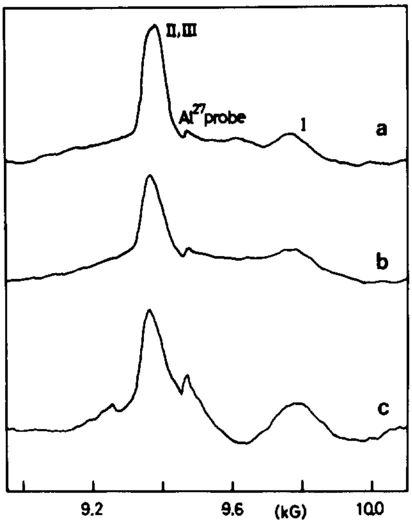

FIG. 3. Integrated NMR profiles of ^{51}V nuclei in $V_{1-x}Ti_xS_{1.57}$ with a 1-kG magnetic field scan at a frequency of 10.5 MHz. The spectra of a, b, and c belong to $x = 0.0$, 0.2, and 0.5, respectively. Nearly centered peaks at about 9.4 kG (type 2) originate from the vanadiums at the V_{II} and V_{III} sites in the metal-full layers and broad peaks at about 9.8 kG (type 1) are due to the vanadiums at the V_I sites in the metal-deficient layers.

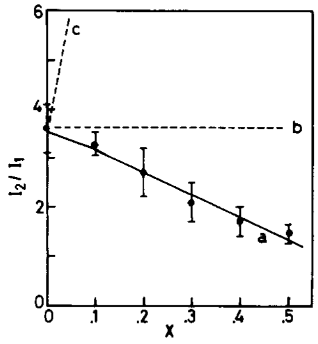

FIG. 4. Composition dependence of the relative intensity ratio between type 2 and type 1 peaks of NMR absorption. The solid and dashed lines represent the ratio between the number of vanadium atoms in the metal-full layers and in the metal-deficient layers calculated in terms of respective site-distribution models of Ti and V as described in the literature.

have itinerant *d*-electrons. The other, called the type 1 peak, is the highly shifted, broad peak observed at about 9.8 kG which originates from the vanadium at the V_I sites in the metal-deficient layers which have localized *d*-electrons (*17–19*). The intensity ratio between type 2 and type 1 peaks is about 3.6 for $x = 0$, the value being nearly equal to the ratio 3.55, between the number of vanadium atoms in the metal-full layers and in the metal-deficient layers for $VS_{1.56}$. The composition dependence of the intensity ratio in the composition range between $x = 0$ and $x = 0.5$ (the metal-excess CdI_2-type phase) is shown in Fig. 4, where the solid line marked *a* is the calculated ratio between the number of vanadium atoms in the metal-full layers and in the metal-deficient layers, assuming that Ti atoms preferably substitute for vanadium atoms in the metal-full layers. The dashed line marked *b* corresponds to the case of random site distribution between metal-full layers and metal-deficient layers; the dashed line marked *c* corresponds to the case that Ti atoms preferably go into the metal sites in the metal-deficient layers. The experimental result clearly agrees with case *a* and disagrees with cases *b* and *c*. Thus Ti atoms preferentially substitute on the metal sites in the metal-full layers of the V_5S_8 phase and the metal-excess CdI_2 phase.

By using a higher frequency (20.8 MHz), the peaks observed at about 9.4 kG in Fig. 3 (type 2) can be resolved as shown in Fig. 5, into two peaks originating from vanadium atoms at the V_{II} and V_{III} sites of the V_5S_8 structure. The low-field peak (see the case for $x = 0$ in Fig. 5) corresponds to the vanadiums at the V_{II} sites and the other corresponds to vanadiums at the V_{III} sites, according to the previous assignment (*16*). Shoulders observed in each main peak for $VS_{1.56}$ are probably due to nonstoichiometry because an almost stoichiometric compound of $VS_{1.59}$ does not show such shoulders, as seen in Fig. 5. The peak from the V_{III} sites, which has intensity nearly equal to that of the V_{II} sites at composition $x = 0$, decreases in intensity rapidly with increasing x and, at the composition $x = 0.3$, the

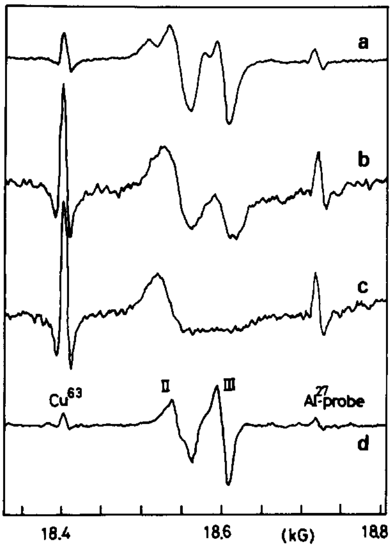

FIG. 5. NMR profiles of ^{51}V nuclei in $V_{1-x}Ti_xS_{1.57}$ with a 500-G magnetic field scan at a frequency of 20.8 MHz. The spectra marked *a*, *b*, and *c* belong to the compositions of $x = 0.0$, $x = 0.1$, and $x = 0.3$, respectively. The spectrum marked *d* belongs to $VS_{1.59}$, that is, almost stoichiometric V_5S_8.

peak is not observed clearly, as shown in Fig. 5. This fact may indicate that Ti atoms preferably substitute for vanadium atoms at V_{III} sites among the metal sites in the metal-full layers until the composition increases near $x = 0.4$, at which point the V_5S_8 structure changes into the metal-excess CdI_2 structure. The value $x = 0.4$ corresponds to the number of V_{III} sites per formula unit of $VS_{1.57}$.

Discussion

The fact that Ti atoms preferably substitute for the metal sites in the metal-full layers more than do V atoms agrees with previous observations in $V_{1-x}Ti_xS_{1.40}$ (*2*). The reason why Ti atoms preferably occupy metal sites in the metal-full layers is made clear through consideration of the crystal structures as was discussed in the study of $V_{1-x}Ti_xS_{1.40}$. In the V_5S_8 structure, a V_{II} site in the metal-full layers has one metal vacancy and one vanadium atom as its neighbors along the *c* axis. A V_{III} site in the metal-full layers has two metal vacancies as neighbors along the *c* axis. On the other hand, the V_I site must have two neighbor vanadium atoms at V_{II} sites in the filled adjacent layers. Therefore, if Ti atoms have a larger repulsive energy resulting from metal–metal interactions of the face-shared octahedra than do V atoms, Ti atoms will substitute in the metal-full layers in preference to the metal-deficient layers, thus decreasing the repulsive energy of the metal–metal interaction along the *c* axis. According to this assumption, Ti atoms should occupy the V_{III} sites first among the three sorts of metal sites, an expectation that agrees with the present observation. A large repulsive energy of the metal–metal interaction of Ti atoms is supported by the following facts: TiS has the largest *c*/*a* ratio (1.94) among 3 *d*-transition metal sulfides with NiAs-like structures, and titanium sulfides of intermediate compositions between TiS and TiS_2 have a variety of sulfur packings modified from the hexagonal close-packed one, resulting in a decrease in the number of face-shared octahedra.

It seems that the phase relations of $V_{1-x}Ti_xS_{1.57}$ are closely related to the site distribution of Ti and V atoms and may be understood by considering the metal–metal interactions along the *c* axis. Ti atoms, at first, substitute for V atoms at the V_{III} sites and then, once they begin to occupy the V_{II} sites after filling almost all the V_{III} sites, the structure of V_5S_8 changes into the metal-excess CdI_2 structure where the V_{II} and V_{III} sites cannot be distinguished. It cannot be understood directly by considering the metal–metal interaction why the structure change occurs at the composition $x = 0.4$. However, the Ti–V repulsive energy of the face-shared octahedra will produce local distortions in the structure and may destroy the ordered state of metal vacancies within the metal-deficient layers, causing phase transition. The local distortion can be understood by considering the local elongation of metal distances along the *c* axis between the Ti–Ti, Ti–V, and V–V distances as discussed previously (*2*). After Ti atoms occupy almost all the metal sites in the metal-full layers of the metal-excess CdI_2 structure ($x = 0.8$), they must begin to substitute for V atoms at the V_I sites, causing a large repulsive energy because of the Ti–Ti interaction. To avoid this situation, the sulfur packing changes from AB type to ABAC type, decreasing the number of face-shared octahedra, and resulting in occurrence of the Ti_2S_3 phase. Thus the site distribution and the metal–metal interaction along the *c* axis may play an important role in determining the phase boundaries and the structures of the system $V_{1-x}Ti_xS_{1.57}$.

Finally, we discuss the reason why Ti atoms would be expected to have a larger repulsive energy than V atoms. The repulsive energy is mainly due to the repulsive Coulomb potential between metal atoms of the face-shared octahedra. Although the repulsive energy may be largely affected by the electronegativity difference between Ti (or V) and S, the metal–metal bonds along the *c* axis may also be important in the ternary Ti–V–S system. These bonds decrease the Coulomb energy through screening by the conduction electrons and contribute to the stability of the structure. It has been observed in a magnetic study of $V_{1-x}Ti_xS_{1.40}$ that localized magnetic moments are produced on V atoms in the metal-deficient layers when the V atoms have two Ti neighbors along the *c* axis (*2*). This observation suggests that substitution of Ti for V probably weakens the metal–metal bonding along the *c* axis, causing localization of the *d*-electrons. In the VS–VS_2 system, the metallic bond along the *c* axis may contribute to stability of the compounds more significantly than in TiS–TiS_2.

Acknowledgments

The authors are grateful to Professor M. Nakahira for helpful discussion and to Dr. I. Kawada for his support during the present study.

References

1. E. Tronc and R. Moret, *J. Solid State Chem.* **36,** 97 (1981).
2. H. Nozaki, *Mater. Res. Bull.* **16,** 861 (1981).
3. I. Kawada, M. Nakano-Onoda, M. Ishii, M. Saeki, and M. Nakahira, *J. Solid State Chem.* **15,** 246 (1975).
4. M. Onoda, M. Saeki, and I. Kawada, *Z. Anorg. Allg. Chem.* **457,** 62 (1979).
5. E. Tronc, R. Moret, J. J. Legendre, and M. Huber, *Acta Crystallogr. Sect. B* **31,** 2800 (1975).
6. F. Jellinek, *Ark. Kemi* **20,** 447 (1963).
7. M. Saeki and M. Onoda, *Bull. Chem. Soc. Japan* **55,** 3144 (1982).
8. M. Saeki and M. Onoda, *Bull. Chem. Soc. Japan* **55,** 113 (1982).
9. M. Saeki, M. Onoda, I. Kawada, and M. Nakahira, *J. Less-Common Met.* **77,** 131 (1981).
10. R. Moret, E. Tronc, M. Huber, and R. Comes, *Philos. Mag. B* **38,** 105 (1978).
11. M. Onoda and M. Saeki, *Acta Crystallogr. B,* in press.
12. Y. Bando, M. Saeki, M. Onoda, I. Kawada, and M. Nakahira, *J. Solid State Chem.* **34,** 381 (1980).
13. M. Saeki, M. Nakano, and M. Nakahira, *J. Cryst. Growth* **24/25,** 154 (1974).
14. M. Saeki, M. Ishii, I. Kawada, and M. Nakahira, *J. Cryst. Growth* **45,** 25 (1978).
15. In Ref. (*2*), the frequency used in NMR experiments was described with an erratum. The correction is that it is not 20.8 MHz but 10.5 MHz.
16. B. G. Silbernagel, R. B. Levy, and F. R. Gamble, *Phys. Rev. B* **11,** 4563 (1975).
17. A. B. de Vries and C. Haas, *J. Phys. Chem. Solids* **34,** 651 (1972).
18. H. Nozaki, M. Umehara, Y. Ishizawa, M. Saeki, T. Mizoguchi, and M. Nakahira, *J. Phys. Chem. Solids* **39,** 851 (1978).
19. S. Funahashi, H. Nozaki, and I. Kawada, *J. Phys. Chem. Solids* **42,** 1009 (1981).